

Influence of Surface Wettability on Droplet Spreading Behaviour over a Solid Substrate

Dhrijit Kumar Deka ¹, Sukumar Pati ¹, László Baranyi ^{2*}

¹ Department of Mechanical Engineering, National Institute of Technology Silchar, Silchar, India-788010

² Department of Fluid and Heat Engineering, Institute of Energy Engineering and Chemical Machinery, University of Miskolc, 3515, Miskolc-Egyetemváros, Hungary

Abstract: The present study investigates the fluid-solid interaction phenomenon when a spherical droplet falls on the surface of a solid substrate. Numerical investigations were carried out in a 2D framework to analyse the influence of the wettability of the substrate and interfacial tension of the liquid droplet. The 2D solver establishes a good agreement with the reported experimental results. The droplet is considered to fall on the solid surface under the influence of a minimal velocity imposed on it. The results are presented in terms of droplet interface morphology and the spreading distance over the solid substrate. It is observed that the spreading tendency of a droplet is much more significant with a hydrophilic surface compared to a hydrophobic surface. It is also established that the droplet spreading increases with the decrease in Weber number. However, droplet spreading on a hydrophobic surface increases with the decrease in Weber number up to a certain limit, after which the droplet starts to contract, reducing the droplet spreading on the surface.

Keywords: Droplet spreading, hydrophilic, hydrophobic, solid substrate, Weber number, wettability.

Nomenclature

D	[mm]	diameter of the droplet
L_s	[-]	non-dimensional spreading length
We	[-]	Weber number
θ	[°]	contact angle
μ	[Pa s]	viscosity
ρ	[kg/m ³]	density
σ	[N/m]	surface tension
τ	[-]	non-dimensional time
$\phi(x, t)$	[-]	level-set function

1 Introduction

When a droplet impacts on a solid surface, the dynamics of interfacial characteristics becomes complex. Researchers have found the dynamics of a droplet impacting on a substrate a topic of interest owing to its appealing physics and versatile applications like ink-jet printing (van Dam and Le Clerc, 2004), pesticide depositions (Massinon and Lebeau, 2012), impact erosion (Oka et al., 2007), anti-icing (Antonini et al., 2011), etc.

Droplet impact on a solid substrate takes many forms e.g., spreading, bouncing, fingering, splashing, etc. (Yarin, 2006) based on different properties of the surface as well as different physiochemical and flow properties of the fluid. These include the surface properties of roughness (Xu, 2007) and wettability (Aboud and Kietzig, 2015), while fluid properties such as interfacial tension, viscosity, density, and impact velocity (Stevens et al., 2014; Roisman et al., 2009; Pasandideh-Fard et al., 1996) are some of the key determinants dictating the droplet impact over a solid surface.

The spreading of a liquid droplet on a specifically wetted surface has drawn attention from the research community for bearing remarkable potential within the domain of biomedical research, microfluidics, lab-on-chip applications, etc. The key parameters that govern the phenomenon of spreading over a solid substrate are dynamic contact angle, impact velocity of the droplet and topology of the solid-liquid contact line. Researchers have reported that the dynamic contact angle is dependent upon the physical structure of the impacting surface (Krishnan et al., 2005), interfacial characteristics of the participating liquid (Strobel and Lyons, 2011) and also the method by which the droplet is let to impact over the surface (Pierce et al., 2008; Brutin et al., 2009).

* E-mail address: laszlo.baranyi@uni-miskolc.hu

doi: [10.24352/UB.OVGU-2023-041](https://doi.org/10.24352/UB.OVGU-2023-041)

2023 | All rights reserved.

Wildeman et al. (2016) investigated numerically and analytically the spreading behaviour of droplet over a smooth surface when the droplet impacts the surface at a high velocity. They found that during the spreading of a liquid droplet over the free-slip surface one-half of the kinetic energy is converted to interfacial energy, irrespective of any other flow parameters. Laan et al. (2014) experimentally explored the influence of impacting droplet diameter on spreading over a solid surface. They reported that the spreading characteristics of the droplet not only depend on the inertia, viscous or capillary force, but also on the droplet size and provide an accurate scaling of droplet spreading behaviour. Léopoldés and Bucknall (2005) identified three distinct regimes of droplet spreading when a solid surface is differentiated with two micro-stripes having definite wettability contrast. In their study, different spreading behaviours of droplet were analysed with the variation of wettability contrast. In another study carried out by Kuznetsov et al. (2016), three different spreading regimes were identified for a distilled water droplet impacting a solid superhydrophobic and copper substrate.

The dynamics of a droplet when it is imposed with a certain velocity can be characterized by a non-dimensional similarity number called Weber number (We), which represents the relative importance of velocity with respect to the surface tension of the liquid. Liu et al. (2019) investigated the spreading characteristics of a droplet over a surface at low Weber numbers. Shang et al. (2020) explored the spreading of a droplet for a range of Weber numbers on a solid surface maintained at a very low temperature. They reported that a low Weber number leads to a decrease in spreading length, with spreading length first decreasing and then increasing with subsequent cooling at higher Weber numbers.

Most of the recent studies on the spreading of a liquid droplet over a solid surface have explored the influence of surface wettability and a few key determinants like impact velocity, viscosity or surface tension. However, the combined effect of surface wettability with a low Weber number on the spreading characteristics is yet to be studied. Thus, the present study aims to investigate the spreading behaviour of a liquid droplet on a solid surface of different wettability conditions for a specific range of Weber numbers.

2 Problem Formulation

The present study numerically investigates the spreading behaviour of a liquid droplet over solid substrate under the combined influence of the wettability condition of the substrate surface, the initial velocity of the droplet and the interfacial tension. A two-dimensional computational domain is used (see Fig. 1) in the present investigation in order to reduce the cost of computation, and it is justified by the fact that the present 2D computational results agree well with reported experimental work, as discussed in Section 3.

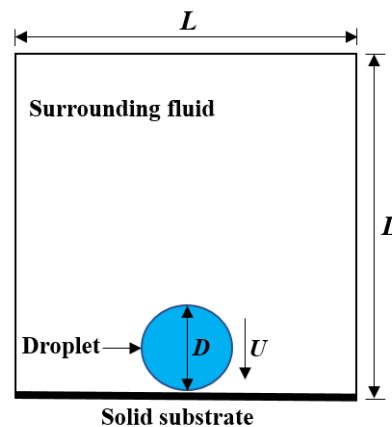


Fig. 2.1: Physical domain of the formulated problem.

The diameter of the droplet (D) is considered to be 2 mm, and based on this; the other dimensions of the computational domain are set. The diameter of the droplet (D) is considered to be 2 mm and based on this; the other dimensions of the computational domain are set. The side length of the square domain is considered to be $L = 10 D$. The droplet is set to fall on the substrate from a distance of $0.01 D$. The liquid droplet is considered to be water (fluid 1) with density (ρ) and viscosity (μ) of 1000 kg/m^3 and 0.001 Pa s , respectively. The water droplet is surrounded by air (fluid 2) ($\rho = 1.22 \text{ kg/m}^3$, $\mu = 1.98 \times 10^{-5} \text{ Pa s}$). The side boundaries are imposed with free-slip boundary conditions, whereas the top boundary of the domain is considered to be of constant pressure identical with the ambient pressure and no-slip boundary conditions are prescribed at the bottom. The effect of gravity is neglected as the size of the droplet is very small (Ristenpart et al., 2006). The initial velocity of the droplet is $U = 0.001 \text{ m/s}$ and the surrounding air is assumed to be stationary. The study puts emphasis on investigating the spreading behaviour changes with different wettability conditions of the wall combined with the interfacial tension of the droplet. Two specific wettability conditions were imposed on the surface: hydrophilic and hydrophobic with a contact angle (θ) of 78 and 150 , respectively. The influence of surface tension (σ) with respect to imposed velocity is measured with a non-dimensional parameter called the Weber number ($We = \rho U^2 D / \sigma$) which was varied within a range of 0.001 - 0.0028 .

Governing equations

The present study adopts the two-phase laminar flow level-set formalism for accurate capturing of interface based on finite element method. For this purpose, an implicit scalar function, the level-set function, is defined to describe the minimum distance of any

location from the interface as

$$\phi(x, t) = \begin{cases} 1 & \text{in the domain of fluid 1} \\ 0 < \phi < 1 & \text{at the interface} \\ 0 & \text{in the domain of fluid 2} \end{cases} \quad (2.1)$$

After defining the level-set function $\phi(x, t)$, a generalised transport equation is solved to track the position of the interface throughout the domain as follows

$$\frac{\partial \phi}{\partial t} + \mathbf{u} \cdot \nabla \phi = \nabla \cdot \left[\lambda \nabla \phi - \phi(1 - \phi) \frac{\nabla \phi}{|\nabla \phi|} \right], \quad (2.2)$$

where, t denotes time, \mathbf{u} represents the velocity field, and λ is the diffusion coefficient, which is the product of parameter controlling interface thickness and a re-initialization parameter.

Next, the level-set function is coupled with the velocity field in order to obtain the coupled Navier-Stokes equation, which can be expressed as

$$\rho \left(\frac{\partial \mathbf{u}}{\partial t} + \mathbf{u} \cdot \nabla \mathbf{u} \right) = -\nabla P + \nabla \cdot [\mu(\nabla \mathbf{u} + \nabla \mathbf{u}^T)] + \sigma \kappa \hat{\mathbf{n}} \delta_s(r - r_\Gamma), \quad (2.3)$$

where P is the pressure, μ is the dynamic viscosity, σ is the fluid to fluid interfacial tension, κ is the curvature of the interface, $\delta_s(r - r_\Gamma)$ is a delta distribution function that is zero everywhere except at the interface and $\hat{\mathbf{n}}$ represents the normal direction to the drop surface. Equations (2.2) and (2.3) are solved with the continuity equation given by

$$\nabla \cdot \mathbf{u} = 0. \quad (2.4)$$

3 Numerical Methodology and Model Validation

The governing equations with the boundary conditions are numerically solved using finite element method (FEM) based solver. The computational domain is divided into certain numbers of sub domains termed as elements. Each of the flow variables and interface positions are approximated using the interpolation functions within these elements. The flow variables within the computational domain are approximated using quadratic Lagrangian basis function. After inserting the approximate field variables into the governing equations, residuals (R) are generated, the weighted average of which becomes zero over the computational domain. The resulting systems of equations are non-linear in character and are solved iteratively until a pre-set residual criterion is satisfied as $\max |(\varepsilon^{n+1} - \varepsilon^n)/\varepsilon^n| \leq 10^{-6}$. Here, ε and n refer to the transport variables and the iteration level, respectively. The present solver was tested for grid independence. Grid independent results were obtained for a grid with 47220 elements. For this grid, the variation of spreading length (L_s) shows a maximum 0.02% relative difference compared to the preceding grid system (with 59262 elements). Table 3.1 shows the comparison of spreading length for different mesh type with varying total number of elements. The entire subsequent investigations are carried out using the grid with total number of elements 47220.

Parameter	Number of elements	Spreading length (L_s)	Relative difference (%)
M1	12398	3.871	3.79
M2	26754	3.724	0.617
M3	47220	3.701	0
M4	59262	3.701	-

Tab. 3.1: Grid independence test at different mesh system (M) showing quantitative comparison of spreading length for different total number of elements. $\theta = 78^\circ$, $We = 0.0028$ and $\tau = 1.5$. The length is normalized by the radius of the droplet.

The mesh used for the present computational investigation is presented in Fig. 3.1, where the fluid-to-solid interacting zone is configured with very fine elements compared to the rest. In the right hand side of Fig. 3.1, the intricate zone as indicated with red square is shown in the zoomed-out version.

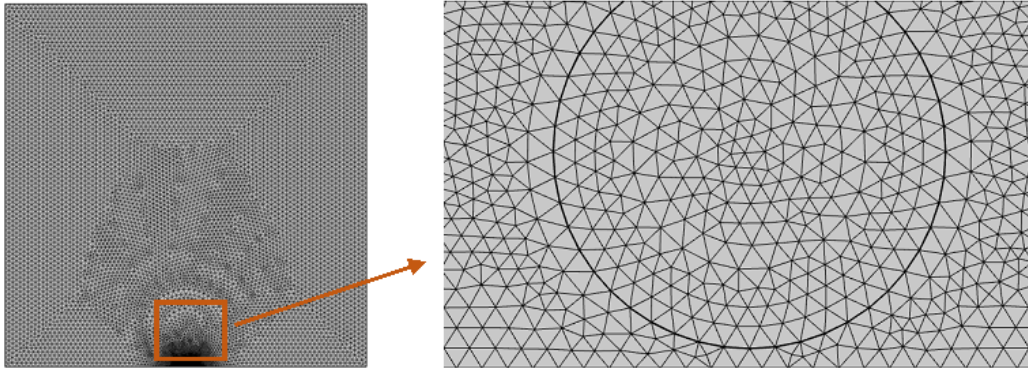


Fig. 3.1: Computational mesh used for the present study.

To test whether the solver is accurate to capture the interfacial dynamics it was used to solve the flow dynamics reported by Lin et al. (2018) in their experimental study where the impact of a droplet over a solid surface with different wettability conditions is extensively analysed. The flow conditions employed in the solver exactly replicated the experimental conditions of Lin et al. (2018). Figure 3.2 compares the results from the solver with those reported by Lin et al. (2018) and finds good agreement. Thus, the present solver is considered to be capable of capturing the interfacial dynamics.

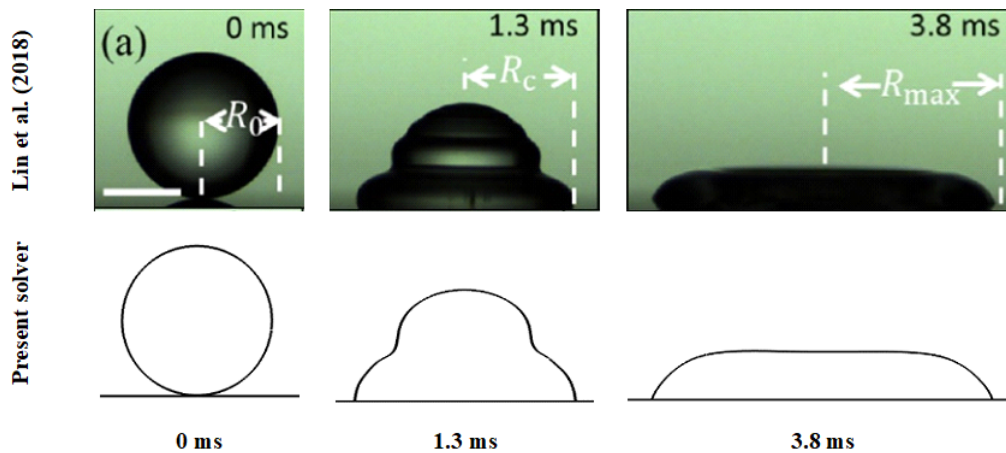


Fig. 3.2: Comparison of results of Lin et al. (2018) and those of the present solver.

4 Results and Discussion

The present study investigates the spreading behaviour of droplet on a surface of a solid substrate. The main aim is to investigate how the spreading characteristics differ with varying wettability conditions of the surface and Weber number. Droplet interface morphology and droplet spreading length are determined for two different surface wettability conditions and a range of Weber numbers. The present study considers only two specific contact angles to represent the two wettability conditions: $\theta = 150^\circ$ for hydrophobic wettability and $\theta = 78^\circ$ for hydrophilic wettability.

Figure 4.1 shows how the droplet interface evolves when it comes in contact with the hydrophilic surface or hydrophobic surface of the solid substrate for the specific Weber number (We) of 0.0028. It can be observed from the figure that the droplet spreads more widely on the hydrophilic surface compared to the hydrophobic surface. On the hydrophilic surface the droplet starts spreading at dimensionless time $\tau = Ut/D = 0.5$ and the solid-liquid interface elongates monotonically. Eventually at $\tau = 1.5$, a capillary wave is formed, which further helps the droplet to spread over the surface and generates a wavy interface, as can be seen at $\tau = 1.5$. Subsequently the wave brings the interface almost parallel to the surface. The hydrophobic surface, however, resists the spreading of the droplet on the surface. The initiation of droplet-to-surface contact lags appreciably, as the droplet is yet to form the liquid-solid interface at $\tau = 0.5$. Once the contact is established, the droplet spreads over the surface with time, although, the spreading length is much smaller than for the hydrophilic surface. This can be illustrated by the fact that the hydrophobic surface has a minimal tendency to accumulate the liquid over it, as the solid surface does not promote spreading of the liquid phase and as a consequence, sideways movement of the droplet over the surface is restricted. In contrast, on the hydrophilic surface, there is a great affinity of the droplet to stick on the surface, due to which the interface spreads along the surface easily.

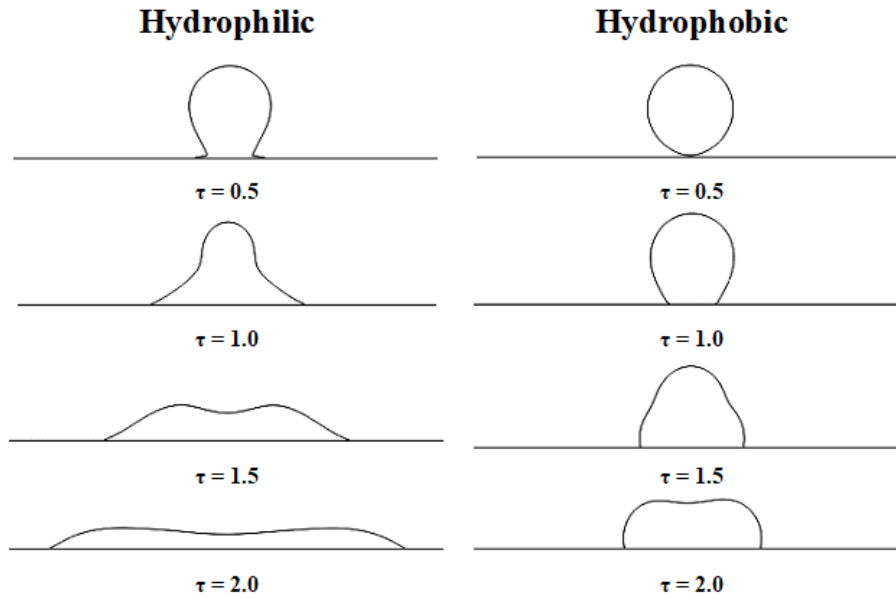


Fig. 4.1: Dynamic evolution of droplet spreading on the solid substrate for two different wettability conditions at $We = 0.0028$.

Figure 4.2 shows the temporal evolution of droplet spreading length on hydrophilic and hydrophobic surfaces. The spreading length (L_s) is normalised by the length of the solid substrate. It is seen in Fig. 4.2 that the spreading length of the droplet for both wettability conditions monotonically increases with time. However, as described in the previous paragraph, for the hydrophobic surface the spreading length is significantly smaller than that for the hydrophilic surface. This is due to the fact that the hydrophilic surface favours for the droplet to spread the surface, whereas, the hydrophobic surface tends to repel the interface from the liquid to solid attachment.

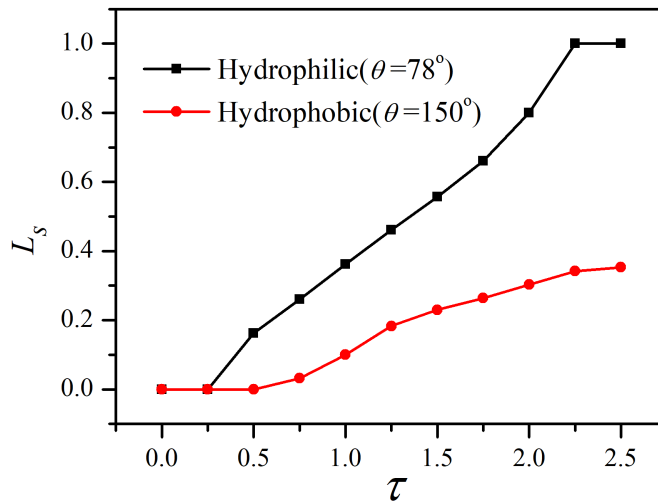


Fig. 4.2: Variation of spreading length (L_s) evolution for hydrophilic and hydrophobic surfaces at $We = 0.0028$.

The spreading behaviour of droplet over a solid surface is highly influenced by the interfacial energy possessed by the droplet. Thus, the present study also explores the different scenarios considering the relative importance of inertia as well as surface tension force that can be expressed through the Weber number. Figure 6 describes the spreading characteristics of a droplet over a hydrophilic surface for three different Weber numbers. For $We = 0.0028$, the droplet starts spreading at $\tau = 0.5$ (Fig. 4.3(a)) and subsequently the spreading length increases as the generated capillary wave pulls the interface laterally. The tip of the droplet shell (seen in Fig. 4.3(b)) becomes smaller under the effect of the capillary wave, and forms a crest in the middle, as can be observed at $\tau = 1.5$ (Fig. 4.3(c)). The wavy interface gradually becomes parallel to the solid substrate, with further spreading along the surface as seen at $\tau = 2.0$ (Fig. 6d). The trend remains similar when the Weber number decreases ($We = 0.002$, $We = 0.001$). However, it can clearly be seen in the figure that with the decrease in Weber number (increasing the surface tension), the spreading tendency increases. It is observed that at any given instant the spreading length is higher for lower values of Weber number. This is due to the fact that the interfacial force aids to the hydrophilicity of the surface and as a cumulative consequence the droplet interface spreads further over the surface. For a hydrophilic surface the droplet interface tends to move towards the surface; when the surface tension increases as We decreases, the droplet interface again maintains the tension in the inward direction and retracts.

Thus, as a cumulative consequence, the interface spreads further over the hydrophilic solid surface with decreasing Weber number. It is interesting to observe that at $We=0.001$, the droplet spreads the most compared to the other Weber numbers and strikes the boundary wall at $\tau = 2.0$ (Fig. 4.3(l)).

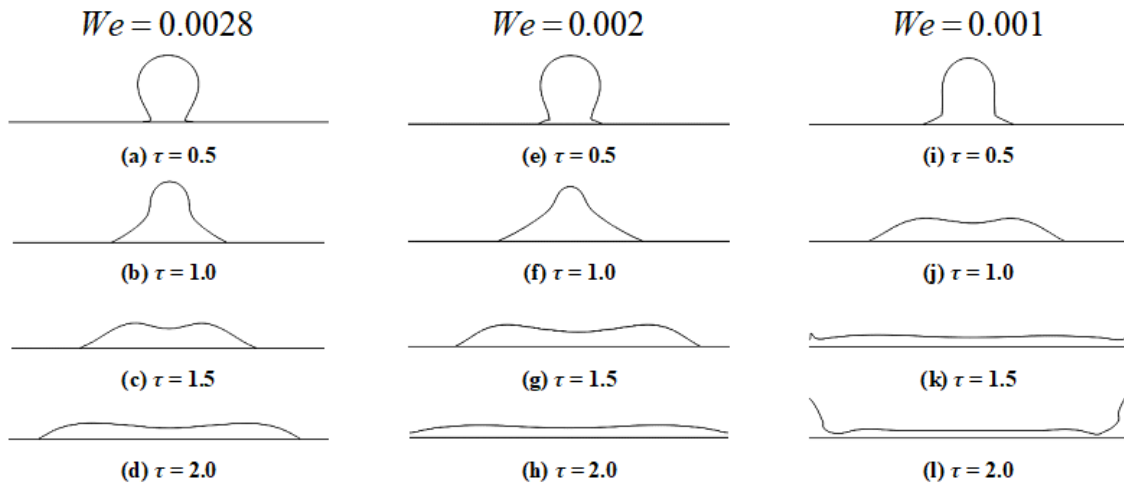


Fig. 4.3: Spreading characteristics of a droplet in terms of interfacial evolution shown at specified instants over a hydrophilic surface for three different We numbers.

Droplet behaviour differs when the solid surface is hydrophobic (with all other conditions kept the same), shown in Fig. 4.4. In a generalised framework it can be observed that for the hydrophobic surface the effect of the capillary wave propagating through the droplet interface is significantly suppressed by the repelling effect of the hydrophobic surface. As a consequence, the crest produced at the middle of the interface is not that remarkable, compared to hydrophilic surface. The concave interface formed in Figs. 4.4(c) & 4.4(f) quickly diminishes, forming a convex interface. It is well known that in case of a hydrophobic surface, the droplet interface is repelled from the surface and thus spreads less, whereas the increasing interfacial tension favours wider spreading of the liquid over the surface. In other words, two forces oppose to each other, meaning that the droplet interface exerts a resisting effect on the way of its expansion over the hydrophobic surface. Although the increasing interfacial tension due to decrease in Weber number provides favourable conditions for spreading, the repelling action of a hydrophobic surface also suppresses the expansion. Thus, at $We = 0.0028$, the droplet spreads gradually over the surface. However, with the decrease in We , the droplet spreads up to a critical limit, a point at which the interfacial tension prevails over the surface repelling of the hydrophobic surface and causes the droplet to retract, thus decreasing the length of spread. The retraction occurs as the hydrophobicity of the surface prevails over the interfacial tension. It can be observed from Fig. 4.4 that for $We = 0.002$, the droplet spreads up to $\tau = 2.0$, and then starts retracting, as can be observed at $\tau = 2.5$. The rebounding of droplet begins earlier, and with further decrease in We as it begins even earlier, at $\tau = 2.0$ for $We = 0.001$ (Fig. 4.4(k)).

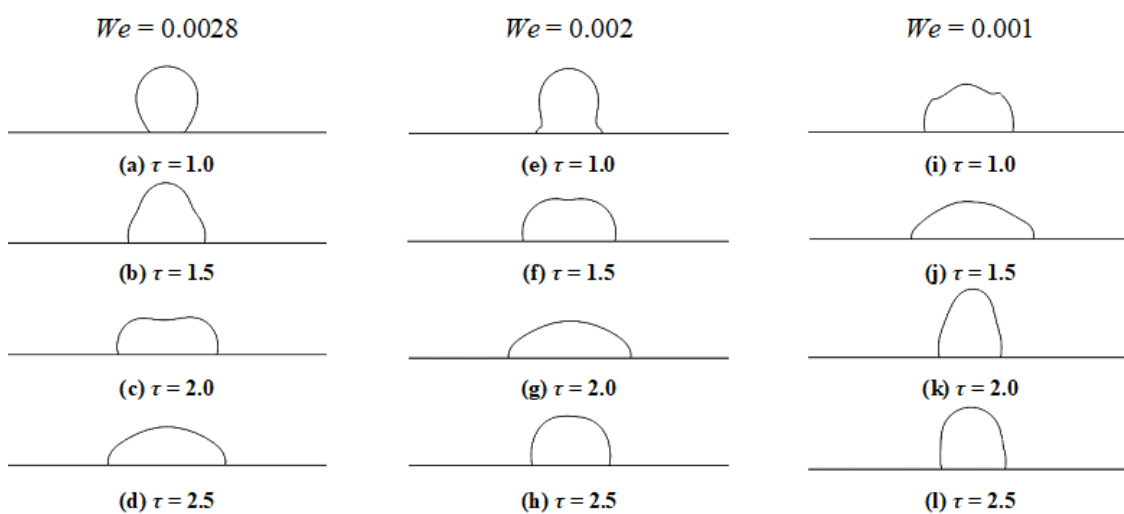


Fig. 4.4: Spreading characteristics of a droplet in terms of interfacial evolution shown at specified instants over a hydrophobic surface for three different We numbers

The spreading behaviour is graphically summarised in Fig. 4.5. With the decrease in We the evolution of spreading length increases as the increasing interfacial tension helps the droplet to spread more over the hydrophilic surface, as shown in Fig. 4.5(a). On the contrary, for the hydrophobic surface shown in Fig. 4.5(b), the spreading length increases up to a critical limit and then starts

decreasing as the droplet interface starts to retract with the decrease in Weber number. The initiation of retraction appears to occur earlier as Weber number decreases.

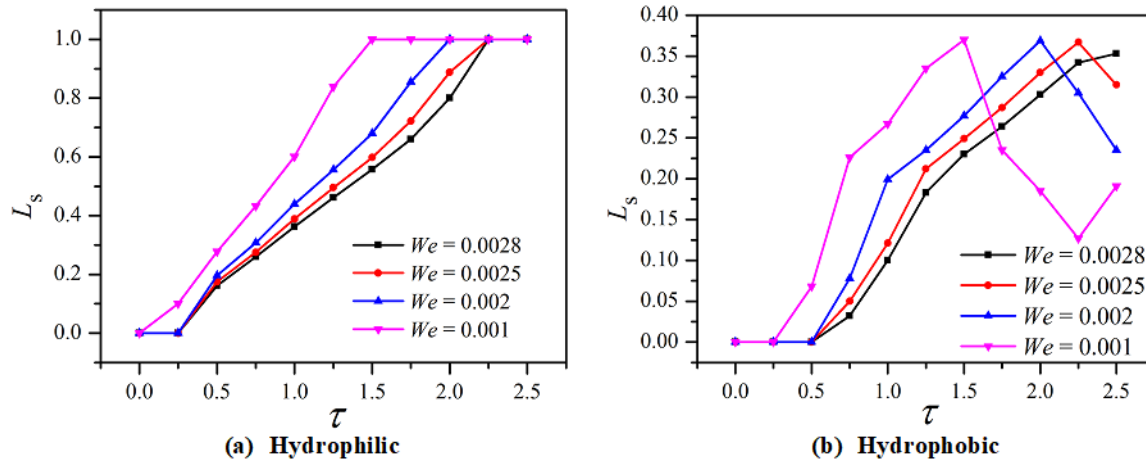


Fig. 4.5: Evolution of spreading length with different Weber numbers (We) over (a) hydrophilic and (b) hydrophobic surface.

5 Conclusions

Two-dimensional numerical investigations were performed to explore droplet spreading characteristics over a solid substrate of different wettability conditions with varying Weber numbers. The outcomes of the study are presented in terms of droplet interface morphology and spreading length evolution under two wettability conditions viz., hydrophilic and hydrophobic along with parametric variations of Weber number. The main findings of the study are as follows.

- The spreading tendency of droplet over the hydrophilic surface is more prominent compared to the hydrophobic surface. The spreading length of the droplet over hydrophilic surface is significantly larger than for hydrophobic surface.
- Decreasing the Weber number results in larger spreading over the hydrophilic surface.
- In the case of the hydrophobic surface, spreading of the droplet increases with decreasing Weber number up to a critical limit, and then the droplet starts to retract. The initiation of retraction over the hydrophobic surface occurs earlier with the decrease in Weber number.

References

- Antonini, C.; Innocenti, M.; Horn, T.; Marengo, M.; Amirfazli, A.: Understanding the effect of superhydrophobic coatings on energy reduction in anti-icing systems. *Cold Reg. Sci. Technol.*, 67, (2011), 58-67.
- Brutin, D.; Zhu, Z.; Rahli, O.; Xie, J.; Liu, Q.; Tadrist, L.: Sessile drop in microgravity: creation, contact angle and interface. *Microgravity Sci. Tec.*, 21, (2009), 67-76.
- Krishnan, A.; Liu, Y. H.; Cha, P.; Woodward, R.; Allara, D.; Vogler, E. A.: An evaluation of methods for contact angle measurement. *Colloid. Surface. B*, 43, (2005), 95-98.
- Kuznetsov, G. V.; Feoktistov, D. V.; Orlova, E. G.: Regimes of spreading of a water droplet over substrates with varying wettability. *J. Eng. Phys. Thermophys.*, 89, (2016), 317-322.
- Laan, N.; de Bruin, K. G.; Bartolo, D.; Josserand, C.; Bonn, D.: Maximum diameter of impacting liquid droplets. *Phys. Rev. Appl.*, 2, (2014), 044018
- Léopoldés, J.; Bucknall, D. G.: Droplet spreading on microstriped surfaces. *J. Phys. Chem. B*, 109, (2005), 8973-8977.
- Lin, S.; Zhao, B.; Zou, S.; Guo, J.; Wei, Z.; Chen, L.: Impact of viscous droplets on different wettable surfaces: Impact phenomena, the maximum spreading factor, spreading time and post-impact oscillation. *Colloid Interf. Sci.*, 516, (2018), 86-97.
- Liu, X.; Zhang, X.; Min, J.: Spreading of droplets impacting different wettable surfaces at a Weber number close to zero. *Chem. Eng. Sci.*, 207, (2019), 495-503.
- Massinon, M.; Lebeau, F.: Experimental method for the assessment of agricultural spray retention based on high-speed imaging of drop impact on a synthetic superhydrophobic surface. *Biosyst. Eng.*, 112, (2012), 56-64.
- Oka, Y. I.; Mihara, S.; Miyata, H.: Effective parameters for erosion caused by water droplet impingement and applications to surface treatment technology. *Wear*, 263, (2007), 386-394.
- Pasandideh-Fard, M.; Qiao, Y. M.; Chandra, S.; Mostaghimi, J.: Capillary effects during droplet impact on a solid surface. *Phys. Fluids*, 8, (1996), 650-659.
- Pierce, E.; Carmona, F. J.; Amirfazli, A.: Understanding of sliding and contact angle results in tilted plate experiments. *Colloid. Surface. A*, 323, (2008), 73-82.
- Ristenpart, W. D.; McCalla, P. M.; Roy, R. V.; Stone, H. A.: Coalescence of spreading droplets on a wettable substrate. *Phys. Rev. Lett.*, 97, (2006), 064501
- Roisman, I. V.; Berberović, E.; Tropea, C.: Inertia dominated drop collisions. I. On the universal flow in the lamella. *Phys. Fluids*, 21, (2009), 052103.

- Shang, Y.; Zhang, Y.; Hou, Y.; Bai, B.; Zhong, X.: Effects of surface subcooling on the spreading dynamics of an impact water droplet. *Phys. Fluids*, 32, (2020), 123309
- Stevens, C. S.; Latka, A.; Nagel, S. R.: Comparison of splashing in high- and low viscosity liquids. *Phys. Rev. E*, 89, (2014), 063006.
- Strobel, M.; Lyons, C. S.: An essay on contact angle measurements. *Plasma Process. Polym.*, 8, (2011), 8-13.
- van Dam, D. B.; Le Clerc, C.: Experimental study of the impact of an ink-jet printed droplet on a solid substrate. *Phys. Fluids*, 16, (2004), 3403-3414.
- Wildeman, S.; Visser, C. W.; Sun, C.; Lohse, D.: On the spreading of impacting drops. *J. Fluid Mech.*, 805, (2016), 636-655.
- Xu, L.: Liquid drop splashing on smooth, rough, and textured surfaces. *Phys. Rev. E*, 75, (2007), 056316
- Yarin, A. L.: Drop impact dynamics: splashing, spreading, receding, bouncing. *Annu. Rev. Fluid Mech.*, 38, (2006), 159-192.